Supplemental Document

Biomedical Optics EXPRESS

Multimodal imaging of metabolic activities for distinguishing subtypes of breast cancer: supplement

ZHI LI,[1] CHLOE NGUYEN,[1] HONGJE JANG,[1] DAVID HOANG,[1] SOESU MIN,[2] ELLEN ACKERSTAFF,[2] JASON A. KOUTCHER,[2,3,4] AND LINGYAN SHI[1,*]

[1]*Department of Bioengineering, University of California San Diego, California, USA*
[2]*Department of Medical Physics, Memorial Sloan Kettering Cancer Center, New York, USA*
[3]*Department of Medicine, Memorial Sloan Kettering Cancer Center, New York, USA*
[4]*Weill Cornell Medical College, Cornell University, New York, USA*
[*]*l2shi@ucsd.edu*

Supplement DOI: https://doi.org/10.6084/m9.figshare.24212157

Parent Article DOI: https://doi.org/10.1364/BOE.500252

Supplemental Data

Cell doubling times (DTs) were calculated from the total cell number counted from well images repeatedly acquired over 4-7 time points per independent experiment (n = 3 for BT-474, and n = 1 for TNBC lines); n denotes the number of well images analyzed (number of wells imaged multiplied by number of time points) and t the number of time points imaged. Tumor volumes were calculated from caliper measurements (N denotes number of tumors per cohort).

The fastest growing cell line was MDA-MB-468 and the non-TNBC control BT-474 grew the slowest. As xenografts, BT-474 grew the slowest (longest DT), while HCC1806 grew the fastest, with the other TNBC tumors growing at similar DT (Table S1). Of note is that for BT-474 a subgroup of tumors grew faster and a 2nd subgroup slower. Hence, 2 tumor doubling times were calculated for BT-474.

Table S1: Cell line characteristics and tumor take and growth.

Cell Line	**Ethnicity**	**TNBC Type**	**Cell DT [h]** Mean (±SE, n, t)	**Take Rate**	**Tumor DT [Days]** Mean (±SE, N)
BT-474	Cauc	Non-TNBC	84.0 (±5.8, 42, 7) 93.9 (±5.0, 42, 7) 86.6 (±2.5, 42, 7)	10/15	14.2 (±2.8, 5)$_{FastGrowth}$ 18.9 (±3.4, 5)$_{SlowGrowth}$
MDA-MB-231	Cauc	MSL	49.7 (±1.1, 60, 5)	8/8*	8.72 (±0.78, 8)
MDA-MB-468	AA	BL1	32.37 (±0.78, 60, 4)	7/8	9.4 (±3.6, 7)
HCC70	AA	BL2	48.3 (±4.6, 60, 5)	5/5	7.99 (±0.56, 5)
HCC1806	AA	BL2	39.2 (±2.3, 60, 4)	7/7	3.65 (±0.24, 7)

* 1/8 intradermal

Table S2. Biological assignments of Raman peaks.

Observed peak (cm^{-1})	**Assignment**
748	Tryptophan
1400	CH bending
1584	Reduced cytochrome C
2186	Stretching vibration of CD

2730	Stretching vibration of CH, NH and OH
2852	CH_2 symmetric stretch of lipids
2875	CH_2 asymmetric stretch and CH stretch of lipid and protein
2935	CH_2 asymmetric stretch
3063	Stretching vibration of CH and OH

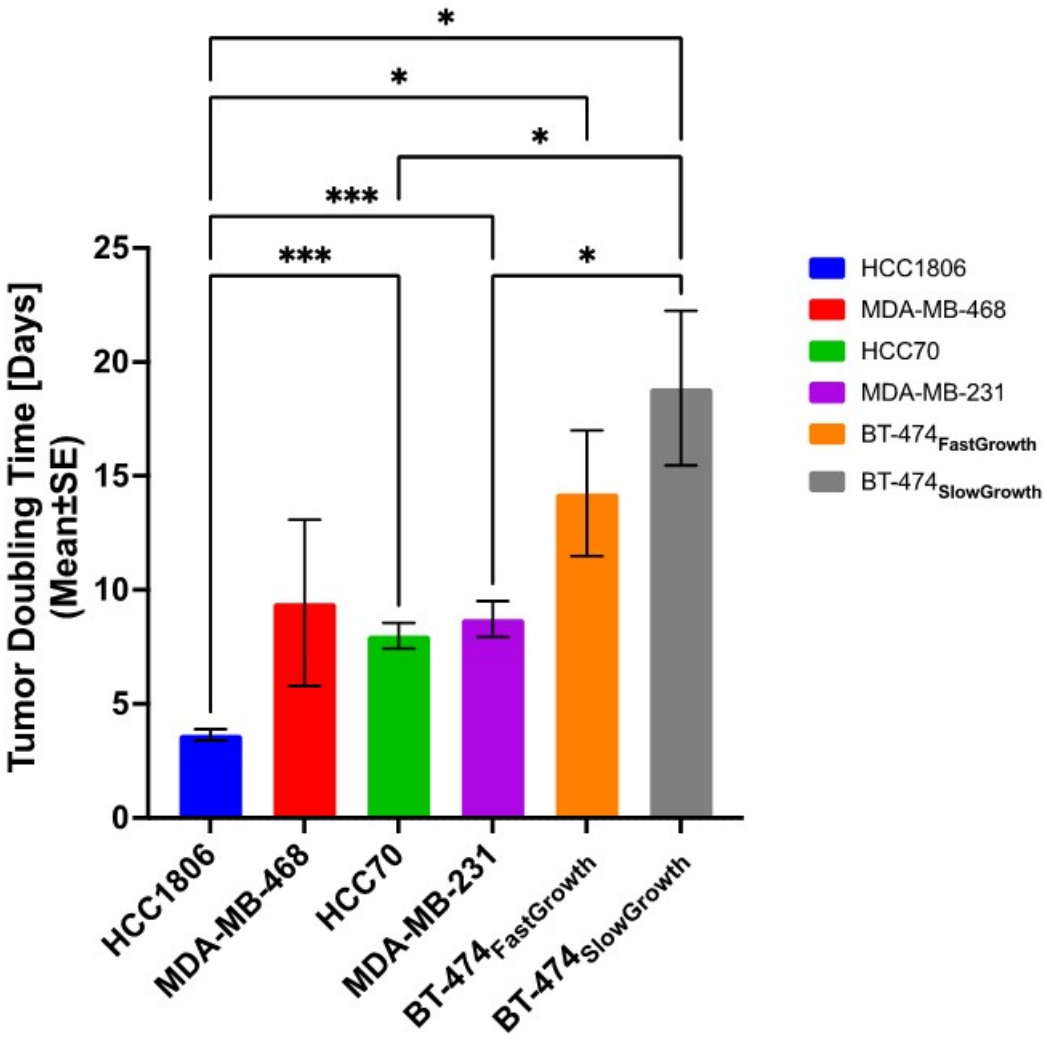

Figure S1. Tumor doubling time. Tumor volumes were calculated from caliper measurements. Statistical significance is determined using two-tailed, unpaired student t-test with Welch's correction.

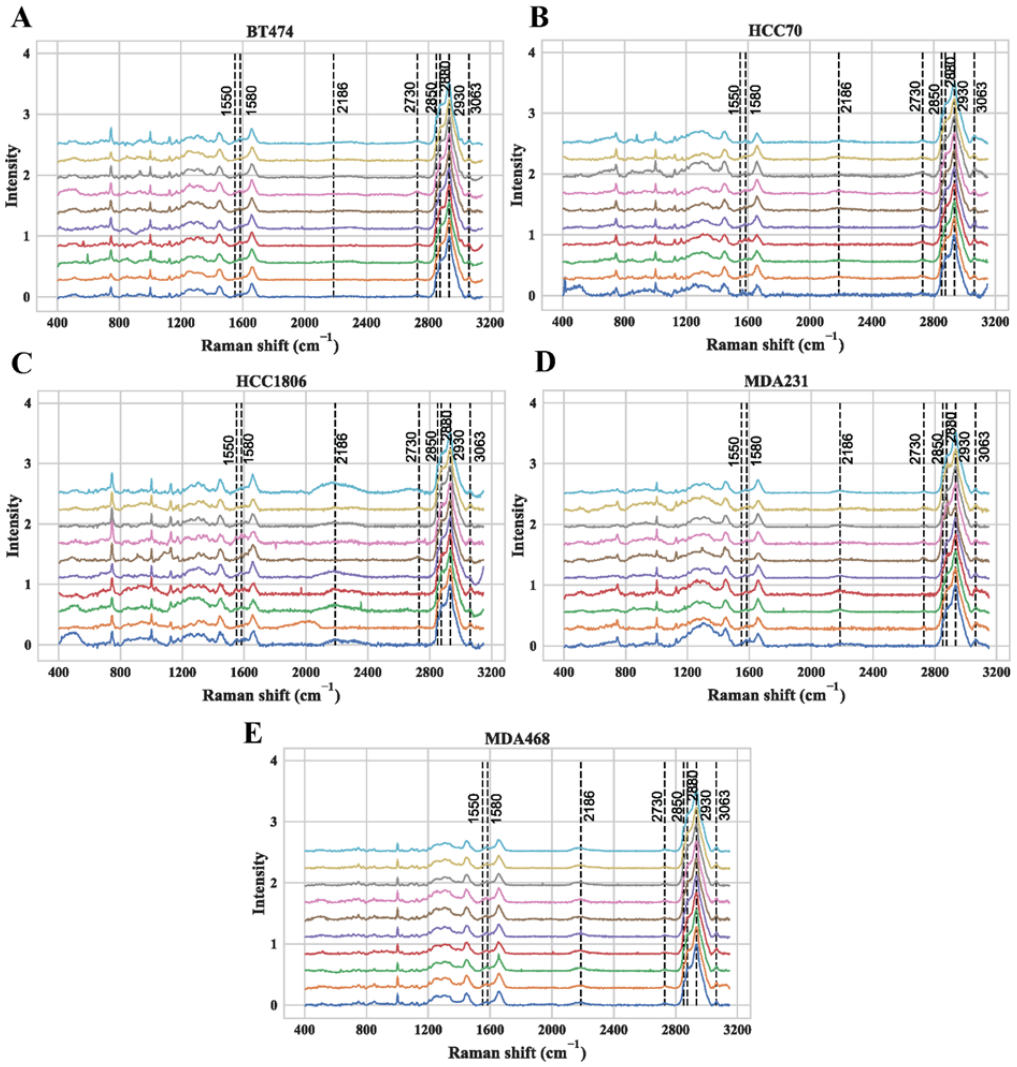

Figure S2. Spontaneous Raman spectra of TNBC subtypes.

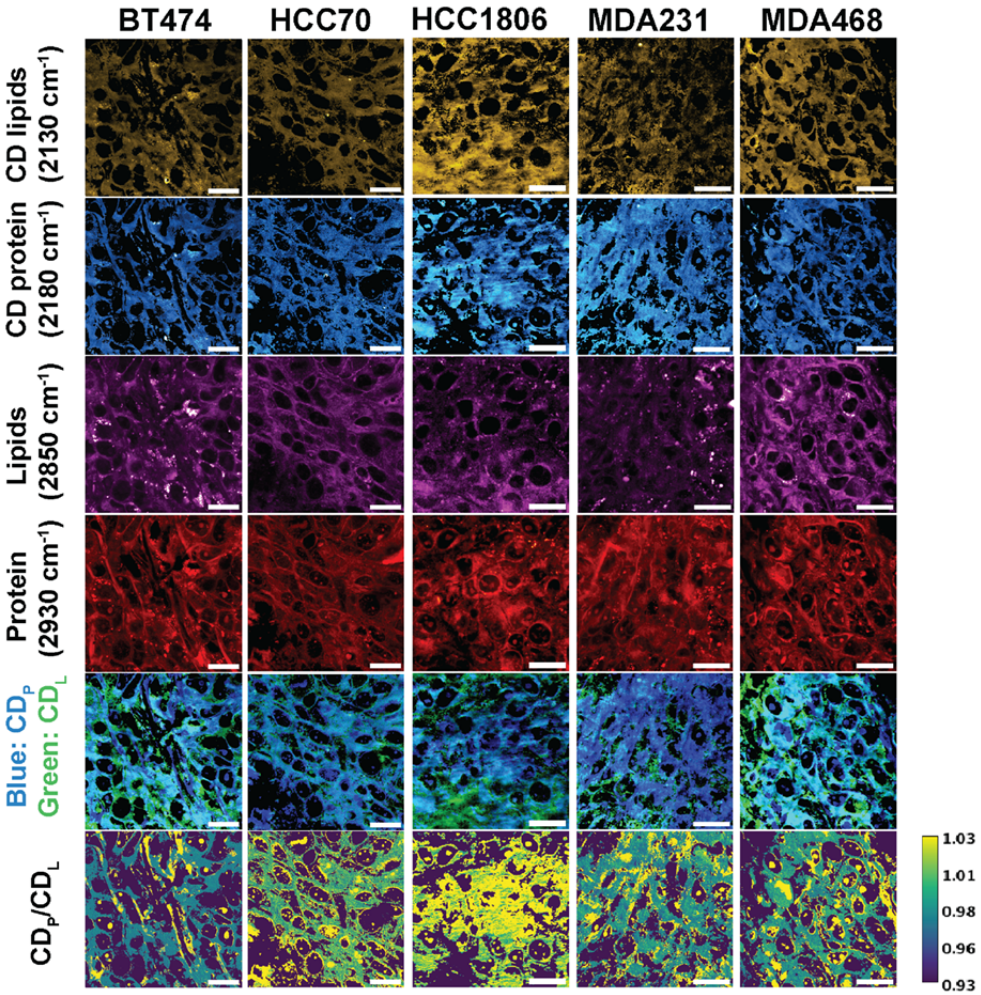

Figure S3. Illustration of de novo protein synthesis and lipogenesis in different breast cancer subtypes. Scale bar: 20 μm.

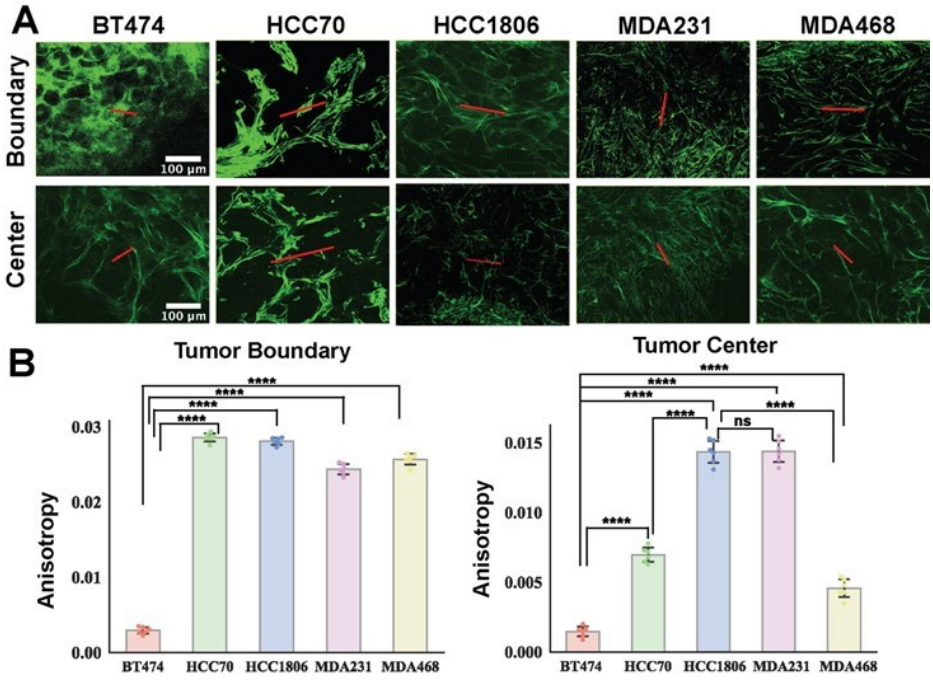

Figure S4. Second harmonic generation (SHG) imaging of collagen fiber in different regions. **(A)** The distribution and orientation of collagen fiber at the boundary and center of tissues, respectively. Scale bar 100 μm. **(B)** Anisotropy analysis of collagen fiber. The anisotropy values of the collagen fiber in TNBC tissues are significantly higher than BT-474 at both the boundary and center of the tissues. For each TNBC subtype, the anisotropy at the tumor boundary was significantly higher than that at the center. Statistical significance was determined by using one-way ANOVA test. ****, $p<0.0001$; ns, non-significant difference.

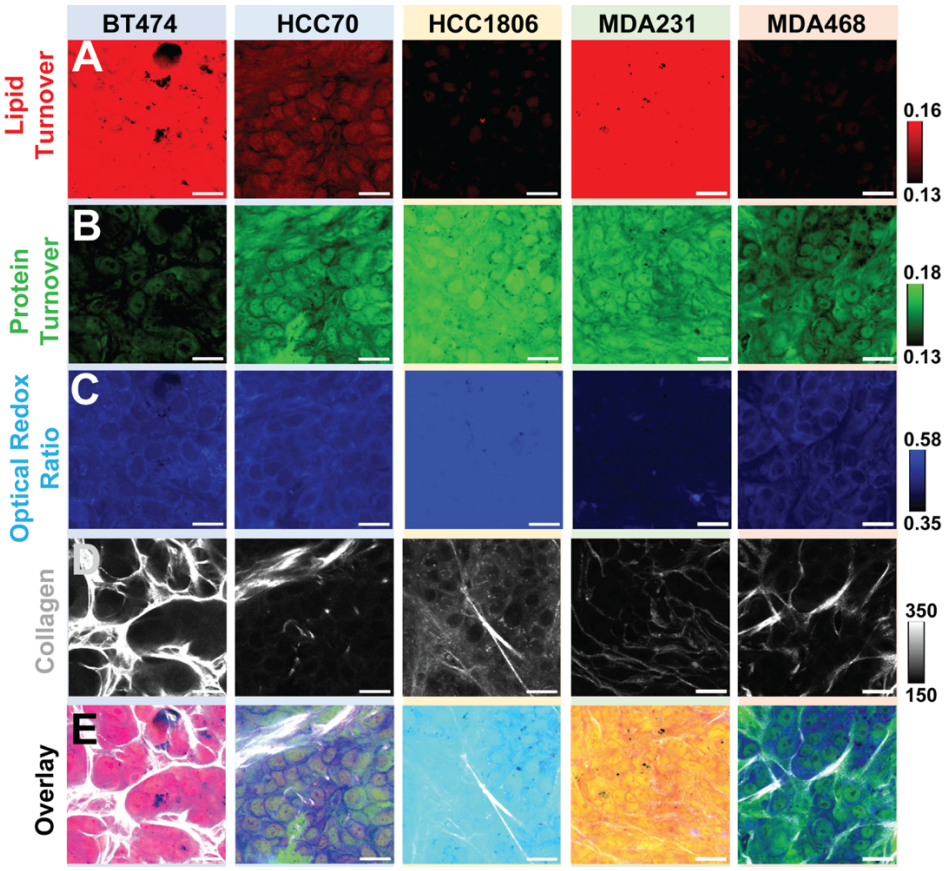

Figure S5. Classification of various TNBC subtypes and non-TNBC through bioorthogonal multimodal imaging. **(A-D)** Illustration of lipid turnover, protein turnover, optical redox ratio, collagen fiber in these subtypes. **(E)** Visualization of overlayed metabolic analysis of various biomarkers discriminates TNBC subtypes. Scale bar: 20 μm.

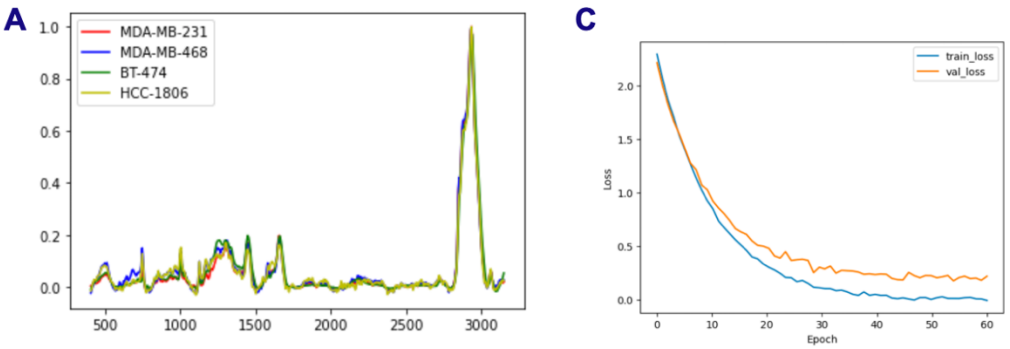

B

	HCC-1806	MDA-MB-468	MDA-MB-231	BT-474
HCC-1806	272	0	4	3
MDA-MB-468	2	243	6	5
MDA-MB-231	4	10	279	9
BT-474	6	4	7	246

Accuracy	Macro Precision	Macro Recall	Macro F1-Score
0.9455	0.9453	0.9458	0.9455

Figure S6. Classification of Raman spectrums of different subtypes using 1D-CNN. (A) Average spectra generated for each TNBC subtype. (B) Confusion matrix with summary of model accuracy after training. (C) Graphical depiction of model loss and accuracy over the course of training.